Clathrate (δ) Form Crystal Transitions of Syndiotactic Polystyrene in Atactic Polystyrene Networks

Xia Gao,[†,‡,§] Ruigang Liu,*[,†] Yong Huang,*[,†] Oleksiy Starykov,[§] and Wilhelm Oppermann[§]

State Key Laboratory of Polymer Physics & Chemistry, Beijing National Laboratory for Molecular Sciences, Institute of Chemistry, Chinese Academy of Sciences, Beijing 100080, China; Beijing Centre of Physical and Chemical Analysis, Beijing Academy of Sciences and Technology, Beijing 100089, China; and Institute of Physical Chemistry, Technical University of Clausthal, Arnold-Sommerfeld Strasse 4, 38678 Clausthal-Zellerfeld, Germany

Received September 4, 2007; Revised Manuscript Received January 29, 2008

ABSTRACT: Syndiotactic polystyrene (sPS) δ crystals within atactic polystyrene (aPS) and atactic polystyrene networks (aPSNW) were prepared. The polymorphism behaviors of sPS within aPS and aPSNW were studied by in-situ wide-angle X-ray diffraction (WAXD) and differential scanning calorimeter (DSC). The sPS δ crystals transfer into γ and then α form crystals during the gradually heating process. The transition temperature of the δ to γ form crystals decreases with the increase in the aPS and aPSNW content in all samples. By contrast, the transition temperature of γ-to-α form crystals increases with the rising aPSNW content, whereas it is independent of the content of aPS. Meanwhile, the transition temperatures of δ to γ and γ to α in aPSNW are higher than those in linear aPS blends. When the samples were annealed at a temperature above 150 °C, the sPS δ form is not favorable to transform into the β form in aPSNW. The results indicate that polymorphism behaviors of sPS are disturbed within aPS networks.

1. Introduction

The crystallization mechanism of polymer within the limited space, including nanospheres, nanorods, and surface area, has received a lot of interest recently.[1–19] The smaller but homogeneous size of the crystallites may give the unusual characteristics in the resultant crystalline structures, which cannot be observed for usual bulk crystals. Some other works focused on the crystallization behaviors within the polymer networks, in which the restricted chain diffusion by the cross-links is a key to emphasize the nucleation effect on polymer crystallization.[20–27] The crystallization of the free linear poly(ethylene oxide) (PEO) chains in poly(trimethopropane trimethacrylate) (PTMPTMA) networks has been reported, which shows the different crystallization behaviors to the bulk state.[27] However, PEO and PTMPTMA network are not miscible, and the crystallization of PEO in the system is somewhat similar to those block copolymer systems.[15–19] On grounds of the published results, there is no clear argument on crystallization behaviors of the linear polymer chains within the miscible networks. The investigations of the crystallization behaviors of linear polymers within their compatible networks might be helpful in this respect.

Syndiotactic polystyrene (sPS) shows a complex polymorphism behavior, and four crystal forms, denoted as α, β, γ, and δ, have been reported.[28–38] Following the nomenclature proposed by Guerra et al.,[38] the crystalline α and β forms are characterized by chains in the *trans* planar conformation, whereas the crystalline γ and δ forms contain chains in the *s*(2/1)2 helical conformation.[28–41] The term δ form has been used to indicate different clathrate structures, that is, compounds which include molecules of solvent. The sPS δ form crystals are generally obtained by the organic solvent induced crystallization from the sPS α, γ, empty clathrate δ crystals, or amorphous state.[36–38,41–43] While being heated gradually, the δ form crystals transfer to γ form crystals at a temperature above the glass transition and then to α form crystals at a temperature around 200 °C.[36–38,44–46] Whereas, sPS β form crystals are formed when the sPS δ form crystals are annealed at a temperature above 150 °C or gradually heated without solvent evaporation.[38,47–49] The characteristic polymorphism of sPS made it possible to be served as the thermoplastic molecular sieves and selective sensors.[50,51]

The crystallization of sPS within its blends has been investigated in the past two decades.[52–57] More recently, the crystallization of sPS within the nanorods has been reported.[58] It was found that α crystals formed for sPS crystallized from amorphous state at lower temperatures, and the degree of crystallinity is the same as that in the bulk. Whereas, for sPS crystallized from molten state at 260 °C, the β crystals formed in the nanorods oriented preferentially with the *c*-axis aligning perpendicular to the axial direction of the nanorod, and the degree of crystallinity was significantly lower than that in the bulk.[58]

In this work, sPS δ form crystals within aPS and aPS network (aPSNW) were prepared. The polymorphism behaviors of sPS within aPS and aPSNW were investigated by in-situ wide-angle X-ray diffraction (WAXD) and differential scanning calorimetry (DSC). Because of that, aPS is miscible with the amorphous state of sPS;[59] this work is helpful for us to understand the influences of the constraining amorphous phase on the crystallization behaviors of linear polymer.

2. Experimental Section

2.1. Materials. Syndiotactic polystyrene (sPS, M_w = 317 000 g/mol, Idemitsu Petrochemical Co. Ltd.) and atactic polystyrene (aPS, M_w = 335 000 g/mol, BASF AG) were used as received. Poly(styrene-*co*-aminomethylstyrene) [P(S-*co*-AMS)] was prepared from aPS by randomly functionalizing with aminomethyl groups. The mole ratio of aminomethyl groups in P(S-*co*-AMS) to the repeat units of aPS is 1:30. The details of P(S-*co*-AMS) synthesis are shown elsewhere.[60]

2.2. Sample Preparation. In the preparation of sPS/aPS network blends, sPS and P(S-*co*-AMS) (totally 0.5 g) were mixed with

* To whom correspondence should be addressed: Tel +086-10-82618573; e-mail rgliu@iccas.ac.cn (R.L.), yhuang@iccas.ac.cn (Y.H.).
† State Key Laboratory of Polymer Physics & Chemistry.
‡ Beijing Centre of Physical and Chemical Analysis.
§ Technical University of Clausthal.

10.1021/ma701988w CCC: $40.75
Published on Web 03/08/2008

Table 1. Content of sPS in Samples and Their Denotation

	denotation of the samples	
contents of sPS (wt %)	sPS/aPS	sPS/aPSNW
100	100	100
80	180	280
60	160	260
50	150	250
40	140	240
20	120	220

toluene (8 mL) in a sealed test tube. The mixtures were heated to 110 °C with continuously stirring until homogeneous solutions were obtained. Then 2 mL of terephthaldialdehyde solution in toluene was added with continuous stirring, by which homogeneous solutions were obtained within 10 s. The aldehyde groups in terephthaldialdehyde are equal to the aminomethyl groups in P(S-*co*-AMS) in molar ratio. The homogeneous solutions were quenched to room temperature, and macrogels formed within several minutes. The samples were kept at room temperature in the sealed test tubes for 1 week and then dried at 90 °C under vacuum until to a constant weight. These samples are denoted as sPS/aPSNW. The sPS/aPS blend samples were prepared by a similar procedure, whereas P(S-*co*-AMS) was replaced by aPS. Generally, it takes tens of minutes to obtain aPS gel by cross-linking P(S-*co*-AMS) with terephthaldialdehyde,[61] which is much slower than the formation of sPS physical gels, δ form crystals, that finished within several minutes. Therefore, in the case of sPS/aPSNW samples, the sPS δ crystals form first and then are surrounded by aPS cross-linked chains. The details of the sample reparation and denotation are summarized in Table 1.

2.3. Measurements. Differential scanning calorimetry (DSC) experiments were performed on a Perkin-Elmer DSC-7 instrument at a heating rate of 10 °C/min under nitrogen. The thermogravimetric analysis (TGA) was carried out on a Perkin-Elmer thermogravimetric analyzer (Pyris 1 TGA) in N_2 atmosphere (20 mL/min) at a heating rate of 10 °C/min. The samples were scanned from 30 to 500 °C.

Wide-angle X-ray diffraction (WAXD) measurements were performed on Bruker D8-Advance X-ray powder diffractometer with a General Area Detector Diffraction System (GADDS). A Cu Kα radiation (λ = 1.542 Å) was used as the X-ray source. The scanning time for each frame was 60 s, and the interval time between two successive measurements was 30 s. The integrated 2θ angle ranged from 5° to 30°. A home-designed hot stage with a Pt-100 thermal couple was used to control the temperature of the samples.

3. Results and Discussion

The characteristic diffraction peaks are at 2θ = 6.7°, 11.8°, 13.5°, and 20.4° for α form, 2θ = 6.1°, 10.4°, 12.2°, 13.6°, 18.5°, and 20.2° for β form, 2θ = 7.8°, 10.2°, 17.2°, 19.7°, and 23.3° for sPS δ form, and 2θ = 9.2°, 15.9° and 20.0° for γ form.[38] Figure 1a shows a typical 3D WAXD pattern for samples heated from 70 to 230 °C with a heating rate of 2 °C/min. The results show the characteristic WAXD pattern of the sPS δ, γ, and α form crystals appears sequentially during the gradually heating procedure, which indicates that the sPS δ form crystals transfer into γ form and then into α form crystals. The polymorphism transition of the sPS δ crystals were further confirmed by the 2D WAXD pattern (Figure 1b), from which the polymorphism transition of sPS during the heating process can be clearly recognized (dotted lines).

The intensity of the characteristic diffraction peaks of sPS δ, γ, and α crystals was recorded during the heating process at a heating rate of 2 °C/min, and the selected typical diffraction intensity profiles and the corresponding derivations are depicted in Figure 2 as a function of temperature. The data for the diffraction peaks at 2θ = 7.8°, 9.2°, and 6.7° correspond to the sPS δ, γ, and α form crystals, respectively. The decrease in

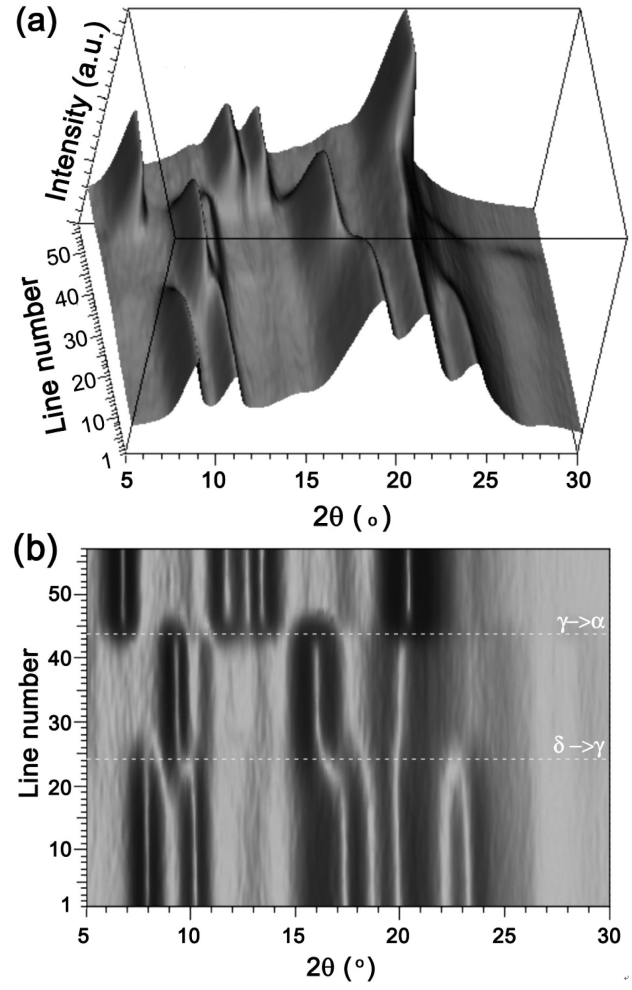

Figure 1. Typical 3D (a) and 2D (b) WAXD pattern of the samples at a heating rate of 2 °C/min.

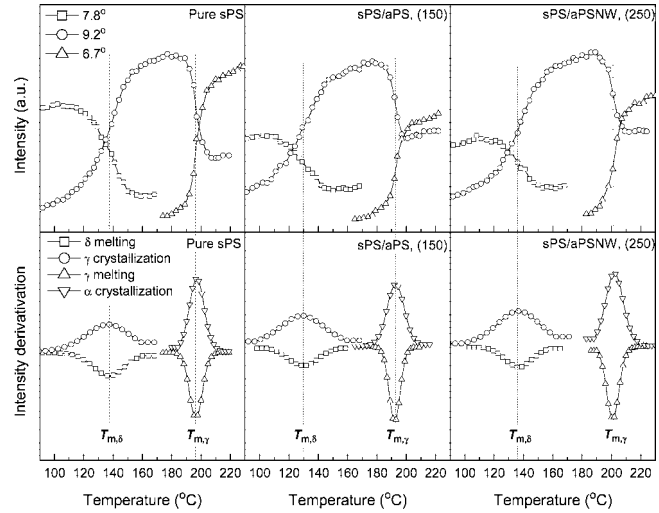

Figure 2. Typical diffraction intensity profiles and corresponding derivation profiles as a function of temperature at the diffraction peaks of 2θ = 7.8°, 9.2°, and 6.7° for sPS δ, γ, and α crystals, respectively.

the diffraction intensity at 2θ = 7.8° and the simultaneous increase in the diffraction intensity at 2θ = 9.2° in the temperature range 100–150 °C are attributed to the melting of the sPS δ form crystals and the crystallization of the sPS γ form crystals, respectively. Similarly, the decrease in the diffraction intensity at 2θ = 9.2° and the increase in the

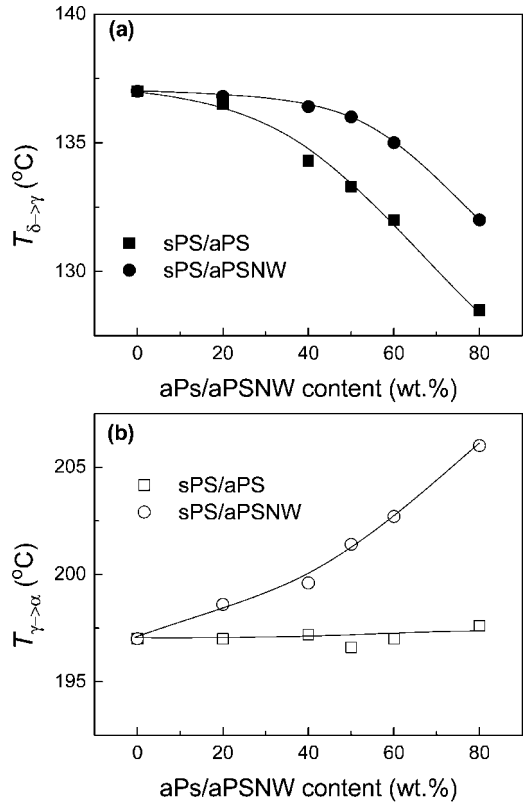

Figure 3. Transition temperatures of sPS δ to γ and γ to α form crystals as a function of aPS or aPSNW content in the samples. The heating rate was 2 °C/min.

diffraction intensity at $2\theta = 6.7°$ at the temperature around 200 °C come from the melting of the sPS γ form crystals and the crystallization of the sPS α form crystals, respectively (Figure 2, top). The peak position of the diffraction intensity derivation of the melting of the sPS δ and γ form crystals and the crystallization of γ and α form crystals can be defined as the melting temperature of δ and γ form crystals ($T_{m,\delta}$ and $T_{m,\gamma}$, respectively) and the crystallization temperature of sPS γ and α form crystals ($T_{c,\gamma}$ and $T_{c,\alpha}$, respectively) (Figure 2, bottom). The results show that $T_{m,\delta} \approx T_{c,\gamma}$ and $T_{m,\gamma} \approx T_{c,\alpha}$, which suggest that the melting of sPS δ and γ form crystals and the crystallization of sPS γ and α form crystals, respectively, occur simultaneously. In this work, the transition temperature of δ to γ and γ to α form crystals can be defined as $T_{\delta\to\gamma}$ ($\approx T_{m,\delta} \approx T_{c,\gamma}$) and $T_{\gamma\to\alpha}$ ($\approx T_{m,\gamma} \approx T_{c,\alpha}$), respectively.

The dependence of $T_{\delta\to\gamma}$ and $T_{\gamma\to\alpha}$ on the content of aPS or aPSNW in the samples is shown in Figure 3. The results indicate that the $T_{\delta\to\gamma}$ drops with the increase in the aPS or aPSNW content (Figure 3a). The decrease in $T_{\delta\to\gamma}$ with the presence of aPS or aPSNW could attribute to the following two aspects. First, the presence of aPS or aPSNW disturbs the formation of sPS δ crystals, which resulted in the smaller and less perfect sPS δ crystals. Second, the presence of aPS or aPSNW provides more space for the evaporation of complex solvent in sPS δ crystals and leads to a lower $T_{\delta\to\gamma}$. However, the TGA results indicate that the presence of both aPS and aPSNW delay the evaporation of the complex solvent during heating process (Figure 4). Therefore, the depression in $T_{\delta\to\gamma}$ should be attributed to the smaller and less perfect sPS δ crystals by aPS or aPSNW, which is supported by the data listed in Table 2. In Table 2, the full width at half-maximum (fwhm) of sPS δ crystals in sPS/aPS and sPS/aPSNW samples was estimated by fitting the experimental WAXD curves with the PeakFit program (SYSTAT Software Inc.). The crystallite size was given by the Scherrer equation, $L = K\lambda/\beta \cos\theta$, where K is the Scherrer

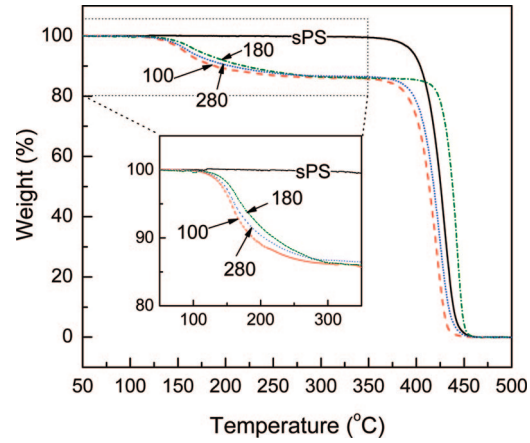

Figure 4. Temperature dependence of weight loss of sPS, sPS δ crystals, sPS/aPS, and sPS/aPSNW.

shape fact and $K = 0.9$ for polymer, λ is the wavelength of X-ray, θ is the Bragg angle, and β is the fwhm in degrees.[62] Generally, a larger value of fwhm corresponds to a less perfection of crystal lattice and visa versa. The results in Table 2 show that the fwhm of sPS/aPS and sPS/aPSNW increases with increasing aPS or aPSNW content, which indicates that the sPS δ crystals become less perfection with increasing aPS or aPSNW content. Moreover, the $T_{\delta\to\gamma}$ in sPS/aPSNW samples is higher than that in sPS/aPS samples with the same aPS or aPSNW content. As described in sample preparation section, the formation of aPS network (gel) is much slower than that of sPS δ crystals.[61] Therefore, the crystallization conditions of sPS in sPS/aPS and sPS/aPSNW are similar during the formation of the sPS δ crystals and the resulted sPS δ crystals have the same level of crystallite perfection. The data listed in Table 2 show that the sPS δ crystals has the similar fwhm values in sPS/aPS and sPS/aPSNW samples with the same aPS or aPSNW content, which indicates that the sPS δ form crystals in both sPS/aPS and sPS/aPSNW samples have the same level of crystal lattice perfection. However, the sPS δ crystals in sPS/aPS blends are surrounded by linear aPS chains, whereas the sPS δ crystals are surrounded cross-linked aPS chains in sPS/aPSNW samples. Furthermore, the complex solvent content, estimated by TGA experiments, in sPS/aPS blends is higher than that in sPS/aPS network samples with the same aPS or aPSNW content (Figure 5). Both the cross-linking state of the aPS chains surrounding the sPS δ crystals and the solvent content in the samples might contribute to the higher $T_{\delta\to\gamma}$ in aPS/aPSNW than that in aPS/aPS blends. Moreover, the sPS chains are all in the **s**(2/1)2 helical conformation with a characteristic periodicity of 7.7 Å in both δ and γ form crystals.[38–41] Therefore, there is no major structure changes during the δ to γ transition. As a result, the cross-linking state of the aPS chain surrounding the sPS δ crystals has a trivial effect on the crystalline transition from δ to γ form. The difference in the content of the complex solvent plays a key role in the higher $T_{\delta\to\gamma}$ in sPS/aPSNW compared to that in sPS/aPS blends.

The transition temperature of sPS γ to α crystal, $T_{\gamma\to\alpha}$, shows a different effect. $T_{\gamma\to\alpha}$ increases with the rising aPSNW content in the samples of sPS/aPSNW, whereas $T_{\gamma\to\alpha}$ is independent of the content of aPS in sPS/aPS blends (Figure 3b). It is known that the sPS chains have the characteristics of s(2/1)2 helical conformation in γ form crystals,[38–41] whereas the sPS chains are in a zigzag planar conformation in α form crystals.[38] As a result, the γ to α transition involves the unraveling of the helices into the linear chains, in which the nature of amorphous phase is important. In the case of sPS/aPSNW, the mobility of sPS chains is restricted by the cross-linked aPS chains, and hence a higher temperature is required for the transition. The higher

Table 2. Full Width at Half-Maxima (fwhm) of sPS δ Crystals within sPS/aPS and sPS/aPSNW

	peak position									
	7.9°		10.2°		17.2°		19.7°		23.3°	
sample	fwhm (deg)	L (nm)	fwhm (deg)	L (nm)	fwhm (deg)	L (nm)	fwhm (deg)	L (nm)	fwhm (deg)	L (nm)
180	1.11	7.17	0.94	8.49	2.46	3.27	2.11	3.82	2.58	3.14
160	1.14	6.99	1.05	7.60	2.45	3.28	2.12	3.80	2.8	2.90
140	1.31	6.08	1.19	6.70	2.69	2.99	2.18	3.70	3.14	2.58
120	1.5	5.31	1.67	4.78	2.91	2.76	2.8	2.88	3.53	2.30
280	1.26	6.32	1.09	7.32	2.57	3.13	2.22	3.63	2.76	2.94
260	1.22	6.53	1.05	7.60	2.62	3.07	2.16	3.73	2.83	2.87
240	1.39	5.73	1.3	6.14	2.63	3.06	2.61	3.09	2.96	2.74
220	1.5	5.31	1.67	4.78	3.11	2.58	2.92	2.76	3.42	2.37

aPSNW content in the sample corresponds to the higher temperature of γ to α crystals transition. In the case of sPS/aPS system, the amorphous phase of sPS and aPS chains having very similar T_g and the temperature of γ to α crystals transition may be independent of aPS content.

Figure 6 shows the DSC heating traces of the samples at a scan rate of 10 °C/min. The broad endothermal peak at 100–160 °C corresponds to the melting of sPS δ crystals, the crystallization of sPS γ crystals, and the evaporation of the complex solvent. Because of that these processes occur simultaneously, as indicated by the above-discussed WAXD and TGA results, the melting temperature of sPS δ crystals $T_{m,\gamma}$ can not be precisely determined by DSC experiments. However, the result clearly shows that the peak position shifts to a lower temperature with the rising aPS or aPSNW content, which also indicates the transition temperature of δ to γ form crystals ($T_{\delta\rightarrow\gamma}$) decreases with the rising aPS or aPSNW content (Figure 6). The overlapped weak endothermal and exothermal peaks at around 200 °C correspond to the melting and the crystallization of the sPS γ and α form crystals, respectively (Figure 6). The result indicates that the transition temperature of the sPS γ to α crystals ($T_{\gamma\rightarrow\alpha}$) increases with rising the content of aPSNW (Figure 6b), whereas the $T_{\gamma\rightarrow\alpha}$ is independent of aPS content in the sPS/aPS blends (Figure 6a). These results are consistent with those of in-situ WAXD results. In DSC experiments, the transition temperature $T_{\delta\rightarrow\gamma}$ and $T_{\gamma\rightarrow\alpha}$ can be estimated as shown by the dotted lines.

In order to have a better understanding on the polymorphism transition of sPS in aPS networks, the fwhm of the selected diffraction peaks is depicted as a function of temperature in Figure 7. The heating rate was set at 2 °C/min. The fwhm at $2\theta = 10.2°$, 9.2°, and 6.7° are selected for sPS δ, γ, and α form crystals, respectively. The results show that when the samples were heated, the value of fwhm at $2\theta = 10.2°$ starts to increase at about 100–130 °C (around T_g of sPS) with rising temperature, which corresponds to the melting of sPS δ crystals and the decrease in the crystal size according to Scherrer equation, $L = K\lambda/\beta \cos\theta$. At about 120–140 °C, the value of fwhm at $2\theta = 9.2°$ decrease dramatically with rising temperature, indicating the formation and growth of sPS γ crystals. While at the temperature around 200 °C, the sPS γ form crystals begin to melt and the sPS α form crystals start to crystallize and growth simultaneously, corresponding to the dramatic increase and decrease in the fwhm value at $2\theta = 9.2°$ and 6.7°, respectively. Moreover, the δ to γ crystal transition process was a relatively slow procedure compared to that of the γ to α transition, which is due to the slow evaporation of the complex solvent during the transition of δ to γ crystals. Unfortunately, it is very difficult to estimate the transition temperatures by the fwhm profiles.

The transition temperatures can be estimated by the WAXD intensity profile at certain diffraction position during heating

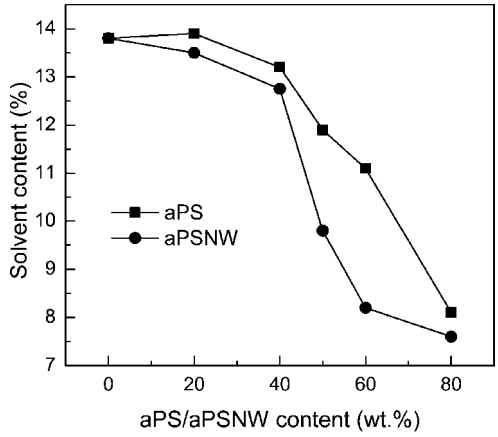

Figure 5. Solvent content as a function of aPS and aPSNW contents. TGA results.

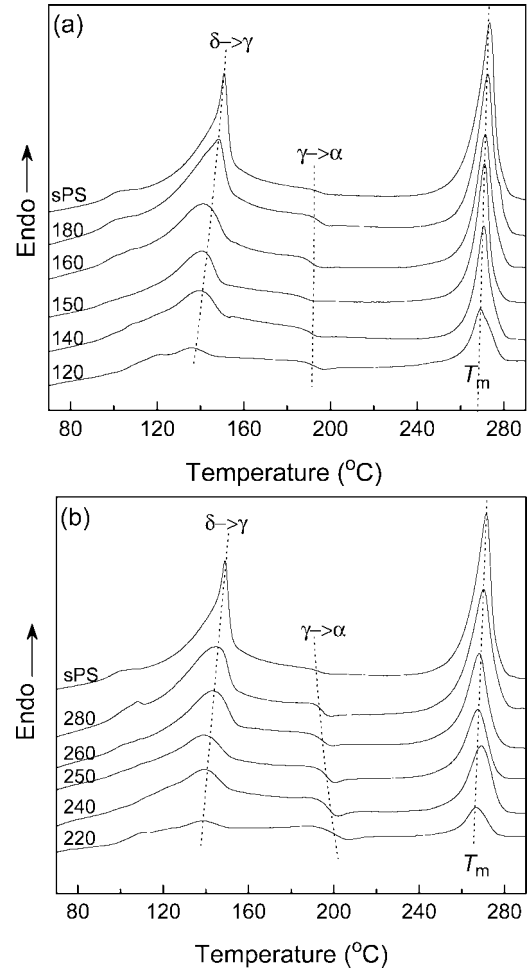

Figure 6. DSC heating traces at 10 °C/min for samples in sPS δ form with different content of aPS or aPS network: (a) sPS/aPS and (b) sPS/aPSNW.

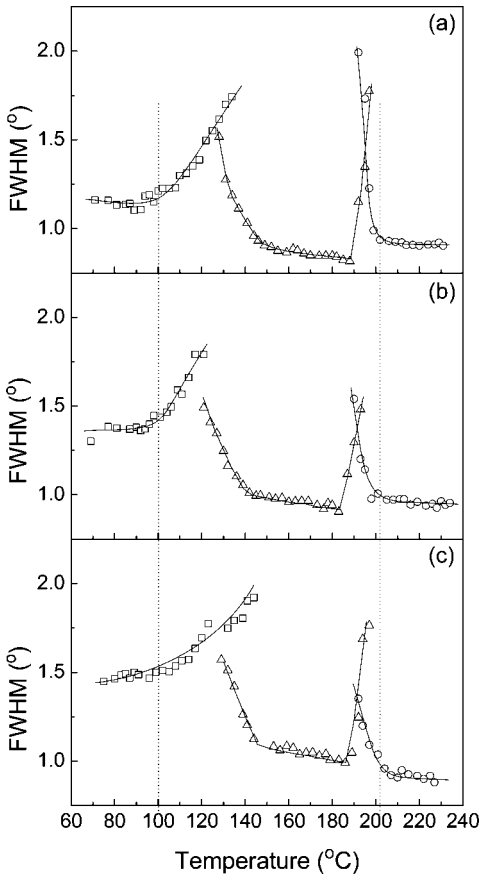

Figure 7. Typical fwhm profiles of sPS δ (□), γ (△), and α (○) crystal forms, at 10.2°, 9.2, and 6.7°, respectively, as a function of temperature during heating with 2 °C/min: (a) sPS, (b) sPS/aPS (50/50, w/w), (c) sPS/aPSNW (50/50, w/w). Lines are used only for guiding the eyes.

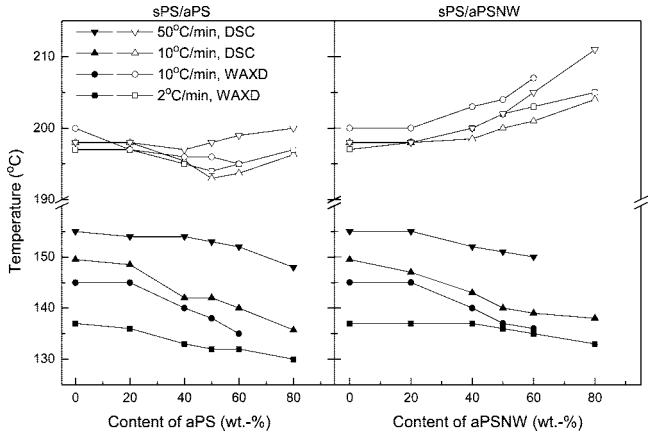

Figure 8. Transition temperature vs the content of aPS and aPSNW obtained by WAXD and DSC with different heating rate. Filled and open symbols stand for $T_{\delta\rightarrow\gamma}$ and $T_{\gamma\rightarrow\alpha}$, respectively.

(Figure 2) or by the DSC experiments (Figure 6). Figure 8 shows the transition temperatures estimated by the WAXD intensity profile at certain diffraction position and DSC analysis at different heating rate. The data have a similar tendency as those in Figure 3. Moreover, the result also shows the $T_{\delta\rightarrow\gamma}$ increases with rising heating rate, whereas the $T_{\gamma\rightarrow\alpha}$ is almost independent of the heating rate, which is due to that the δ to γ transition is a solvent evaporating process and the $T_{\delta\rightarrow\gamma}$ increases with rising heating rate, whereas the γ to α form transition is a melt-recrystallization process and the $T_{\gamma\rightarrow\alpha}$ is independent of the heating rate.[38] Moreover, the $T_{\delta\rightarrow\gamma}$ estimated by DSC measurements is higher than that by WAXD experiments at the same heating rate, which attributes to the fact that samples are half-sealed in the cells in DSC experiments and the evaporation of solvents during heating is hindered somehow, whereas in WAXD experiments, the samples are open to the air. The results also indicate the effect of the solvent evaporation on the transition of δ to γ crystals. Both WAXD and DSC experiments indicate that the surviving window of the sPS γ form crystals becomes wider with the increases in sPS/aPSNW samples.

The above discussions focused on the influences of aPS network on the polymorphism transition of sPS. Figure 9 shows the WAXD curves of the samples obtained by annealing the sPS δ form crystals in sPS/aPS and sPS/aPSNW directly at 150, 180, and 210 °C (Figure 9a−c, respectively). The content of aPS or aPSNW in all the samples is 50 wt %. It has been reported that the sPS β form crystals can be obtained when sPS δ form crystals were annealed at a temperature above 150 °C or gradually heated without solvent evaporation,[38,47–49] which is different from the gradually heating process.[36–38,44–46] In this work, when the samples were annealed at 150 °C for 10 min, only γ form crystal was found in the sPS/aPSNW samples, whereas γ and β form crystals were found in the sPS/aPS blend and there are sPS δ, γ, and β form crystals in the pure sPS (Figure 9a). The results indicate that the presence of aPS leads to the easier transformation of the sPS δ form crystals into the γ and β form crystals, whereas the aPSNW only favorite for the formation of the sPS γ form crystals at the annealing temperature of 150 °C. At the annealing temperature of 180 °C, both γ and β form crystals were found in all the samples (Figure 9b), but the fraction of the sPS β form crystals in pure sPS is higher than that in sPS/aPS and then in sPS/aPSNW blends. At the annealing temperature of 210 °C, a mixture of the sPS α and β form crystals was obtained in both sPS/aPS and sPS/aPSNW samples, whereas only the sPS β form crystal was obtained in the pure sPS samples (Figure 9c). In all cases, the sPS β form crystal appears unfavorable to be obtained in the presence of aPS and aPS networks, especially in the case of sPS/W sample. The result suggests that polymorphism behaviors are disturbed by the confined environment of aPS networks. The sPS β form crystals can be obtained by melt-crystallization depending on the cooling rate, etc.,[38] by isothermal crystallization from a dilute solution,[63,64] by annealing the δ-form,[29] or by casting from solution.[38] In case of annealing sPS as-cast samples from solutions, the planar conformation of sPS β form involves in any event a disorder concerning the molecular packing that is classified as a "stacking fault".[29] The origin of sPS β form crystals may be similar to many isotactic vinyl polymers, which are known to exhibit disorder in molecular arrangement. These disorders are exclusively due to random occupation of one site by either of two kinds of helical polymers that have the same helical sense but differ in directional quality, i.e. up and down senses.[29]

The network morphology of aPS is important to the effect of the polymorphism transition of sPS in aPSNW. Our former work indicated that the aPS gels have a correlation length of tens of nanometers, and the effective chain length between two cross-links is about 10 nm.[60] In this work, the effective chain length between two cross-links may be larger than 10 nm due to that it was disturbed by sPS crystals. The effective cross-linking density of the aPS gels has been estimated by shear modulus and was later confirmed by swelling experiments. However, it is very difficult to estimate the cross-linking density of aPSNW containing sPS crystals by using these methods.

4. Conclusions

Syndiotactic polystyrene (sPS) δ crystals within aPS and aPS networks and sPS blends were prepared. The polymorphism behaviors of sPS within aPS networks and aPS blends were

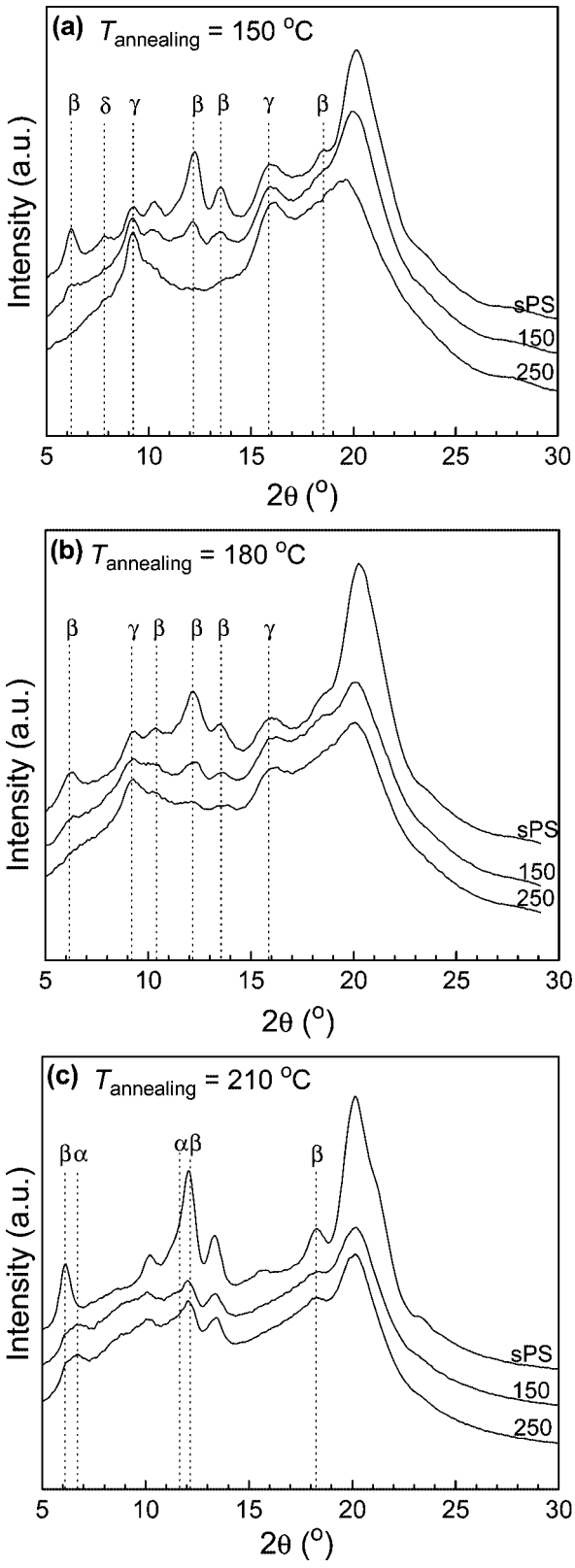

Figure 9. WAXD patterns for sPS δ form samples annealed at (a) 150, (b) 180, and (c) 210 °C for 10 min in the presence of aPS or aPSNW. The content of sPS and aPSNW is 50 wt %.

studied by in-situ wide-angle X-ray diffraction (WAXD) and differential scanning calorimetry (DSC). We found that the transition temperature of sPS δ to γ form crystals decreases with the increase in the aPS or aPSNW content. The temperature of δ to γ transition in sPS/aPSNW is higher than that in sPS/aPS blends with the same aPS content, which attributes to the difference in the content of the complex solvent. The temperature of γ to α transition in sPS/aPSNW samples increases with rising aPSNW content, whereas is independent of aPS content in sPS/aPS blends, which is due to that the nature of the amorphous phase is important to γ to α transition. In the sPS/aPSNW samples, the mobility of sPS chains is restricted by the cross-linked aPS chains, and hence a higher temperature is required for the transition. When the sPS δ form samples were annealed at a temperature above 150 °C, the sPS β form crystal appears unfavorable to be obtained in the presence of aPS and aPS networks, especially in the case of sPS/W sample. The result suggests that polymorphism behaviors are disturbed by the confined environment of aPS networks.

Acknowledgment. The experiments of this work were partially carried out in Technical University of Clausthal. This work was partially supported by the National Natural Scientific Foundation of China (NNSFC) (50521302 and 20634050).

References and Notes

(1) Loo, Y. L.; Register, R. A.; Ryan, A. J. *Phys. Rev. Lett.* **2000**, *84*, 4120–4123.
(2) Massa, M. V.; Dalnoki-Veress, K. *Phys. Rev. Lett.* **2004**, *92*, 255509.
(3) Loo, Y. L.; Register, R. A.; Ryan, A. J.; Dee, G. T. *Macromolecules* **2001**, *34*, 8968–8977.
(4) Shin, K.; Woo, E.; Jeong, Y. G.; Kim, C.; Huh, J.; Kim, K. W. *Macromolecules* **2007**, *40*, 6617–6623.
(5) Weimann, P. A.; Hajduk, D. A.; Chu, C.; Chaffin, K. A.; Brodil, J. C.; Bates, F. S. *J. Polym. Sci., Polym. Phys.* **1999**, *37*, 2053–2068.
(6) Li, C. Y.; Ge, J. J.; Bai, F.; Calhoun, B. H.; Harris, F. W.; Cheng, S. Z. D.; Chien, L. C.; Lotz, B.; Keith, H. D. *Macromolecules* **2001**, *34*, 3634–3641.
(7) Schonherr, H.; Frank, C. W. *Macromolecules* **2003**, *36*, 1199–1208.
(8) Schonherr, H.; Frank, C. W. *Macromolecules* **2003**, *36*, 1188–1198.
(9) Woo, E.; Huh, J.; Jeong, Y. G.; Shin, K. *Phys. Rev. Lett.* **2007**, *98*000.
(10) Steinhart, M.; Senz, S.; Wehrspohn, R. B.; Gosele, U.; Wendorff, J. H. *Macromolecules* **2003**, *36*, 3646–3651.
(11) Steinhart, M.; Goring, P.; Dernaika, H.; Prabhukaran, M.; Gosele, U.; Hempel, E.; Thurn-Albrecht, T. *Phys. Rev. Lett.* **2006**, *97*, 027801.
(12) Massa, M. V.; Carvalho, J. L.; Noki-Veress, K. *Phys. Rev. Lett.* **2006**, *97*, 247802.
(13) Sun, Y. S.; Chung, T. M.; Li, Y. J.; Ho, R. M.; Ko, B. T.; Jeng, U. S.; Lotz, B. *Macromolecules* **2006**, *39*, 5782–5788.
(14) Reiter, G.; Castelein, G.; Sommer, J. U.; Rottele, A.; Thurn-Albrecht, T. *Phys. Rev. Lett.* **2001**, *87*, 226101.
(15) Quiram, D. J.; Register, R. A.; Marchand, G. R.; Adamson, D. H. *Macromolecules* **1998**, *31*, 4891–4898.
(16) Zhu, L.; Cheng, S. Z. D.; Calhoun, B. H.; Ge, Q.; Quirk, R. P.; Thomas, E. L.; Hsiao, B. S.; Yeh, F. J.; Lotz, B. *J. Am. Chem. Soc.* **2000**, *122*, 5957–5967.
(17) Hamley, I. W.; Fairclough, J. P. A.; Ryan, A. J.; Bates, F. S.; TownsAndrews, E. *Polymer* **1996**, *37*, 4425–4429.
(18) Zhu, L.; Huang, P.; Chen, W. Y.; Ge, Q.; Quirk, R. P.; Cheng, S. Z. D.; Thomas, E. L.; Lotz, B.; Hsiao, B. S.; Yeh, F. J.; Liu, L. Z. *Macromolecules* **2002**, *35*, 3553–3562.
(19) Opitz, R.; Lambreva, D. M.; de Jeu, W. H. *Macromolecules* **2002**, *35*, 6930–6936.
(20) Lambert, W. S.; Phillips, P. J.; Lin, J. S. *Polymer* **1994**, *35*, 1809–1818.
(21) Phillips, P. J.; Lambert, W. S. *Macromolecules* **1990**, *23*, 2075–2081.
(22) Phillips, P. J.; Kao, Y. H. *Polymer* **1986**, *27*, 1679–1686.
(23) Takahashi, H.; Shibayama, M.; Hashimoto, M.; Nomura, S. *Macromolecules* **1995**, *28*, 5547–5553.
(24) Shibayama, M.; Takahashi, H.; Yamaguchi, H.; Sakurai, S.; Nomura, S. *Polymer* **1994**, *35*, 2944–2951.
(25) Shibayama, M.; Takahashi, H.; Nomura, S.; Imai, M. *Polymer* **1998**, *39*, 3759–3766.
(26) Qiao, C. D.; Jiang, S. C.; Dong, D. W.; Ji, X. L.; An, L. J.; Jiang, B. Z. *Macromol. Rapid Commun.* **2004**, *25*, 659–663.
(27) Jiang, S. C.; Qiao, C. D.; Tian, S. Z.; Ji, X. L.; An, L. J.; Jiang, B. Z. *Polymer* **2001**, *42*, 5755–5761.
(28) Greis, O.; Xu, Y.; Asano, T.; Petermann, J. *Polymer* **1989**, *30*, 590–594.
(29) Chatani, Y.; Shimane, Y.; Ijitsu, T.; Yukinari, T. *Polymer* **1993**, *34*, 1625–1629.
(30) DeRosa, C. *Macromolecules* **1996**, *29*, 8460–8465.
(31) Tosaka, M.; Hamada, N.; Tsuji, M.; Kohjiya, S. *Macromolecules* **1997**, *30*, 6592–6596.

(32) DeRosa, C.; Rapacciuolo, M.; Guerra, G.; Petraccone, V.; Corradini, P. *Polymer* **1992**, *33*, 1423–1428.
(33) Tarallo, O.; Petraccone, V.; Venditto, V.; Guerra, G. *Polymer* **2006**, *47*, 2402–2410.
(34) Albunia, A. R.; Musto, P.; Guerra, G. *Polymer* **2006**, *47*, 234–242.
(35) Rizzo, P.; Albunia, A. R.; Guerra, G. *Polymer* **2005**, *46*, 9549–9554.
(36) Chatani, Y.; Shimane, Y.; Inoue, Y.; Inagaki, T.; Ishioka, T.; Ijitsu, T.; Yukinari, T. *Polymer* **1992**, *33*, 488–492.
(37) Chatani, Y.; Shimane, Y.; Inagaki, T.; Ijitsu, T.; Yukinari, T.; Shikuma, H. *Polymer* **1993**, *34*, 1620–1624.
(38) Guerra, G.; Vitagliano, V. M.; DeRosa, C.; Petraccone, V.; Corradini, P. *Macromolecules* **1990**, *23*, 1539–1544.
(39) Immirzi, A.; DeCandia, F.; Iannelli, P.; Zambelli, A.; Vittoria, V. *Makromol. Chem., Rapid Commun.* **1988**, *9*, 761–764.
(40) Corradini, P.; Napolitano, R.; Pirozzi, B. *Eur. Polym. J.* **1990**, *26*, 157–161.
(41) De Rosa, C.; Rizzo, P.; de Ballesteros, O. R.; Petraccone, V.; Guerra, G. *Polymer* **1999**, *40*, 2103–2110.
(42) DeRosa, C.; Guerra, G.; Petraccone, V.; Pirozzi, B. *Macromolecules* **1997**, *30*, 4147–4152.
(43) Roels, T.; Deberdt, F.; Berghmans, H. *Macromolecules* **1994**, *27*, 6216–6220.
(44) Gowd, E. B.; Nair, S. S.; Ramesh, C. *Macromolecules* **2002**, *35*, 8509–8514.
(45) Sun, Y. S.; Woo, E. M.; Wu, M. C. *Macromolecules* **2003**, *36*, 8415–8425.
(46) Yoshioka, A.; Tashiro, K. *Macromolecules* **2003**, *36*, 3593–3600.
(47) Rastogi, S.; Goossens, J. G. P.; Lemstra, P. J. *Macromolecules* **1998**, *31*, 2983–2998.
(48) Roels, T.; Rastogi, S.; De Rudder, J.; Berghmans, H. *Macromolecules* **1997**, *30*, 7939–7944.
(49) Malik, S.; Rochas, C.; Guenet, J. M. *Macromolecules* **2005**, *38*, 4888–4893.
(50) Guerra, G.; Milano, G.; Venditto, V.; Musto, P.; De Rosa, C.; Cavallo, L. *Chem. Mater.* **2000**, *12*, 363–368.
(51) Milano, G.; Venditto, V.; Guerra, G.; Cavallo, L.; Ciambelli, P.; Sannino, D. *Chem. Mater.* **2001**, *13*, 1506–1511.
(52) Guerra, G.; DeRosa, C.; Vitagliano, V. M.; Petraccone, V.; Corradini, P. *J. Polym. Sci., Polym. Phys.* **1991**, *29*, 265–271.
(53) Hong, B. K.; Jo, W. H.; Kim, J. *Polymer* **1998**, *39*, 3753–3757.
(54) Cimmino, S.; Dipace, E.; Martuscelli, E.; Silvestre, C. *Polymer* **1993**, *34*, 2799–2803.
(55) Guerra, G.; DeRosa, C.; Vitagliano, V. M.; Petraccone, V.; Corradini, P.; Karasz, F. E. *Polym. Commun.* **1991**, *32*, 30–32.
(56) Park, J. Y.; Kwon, M. H.; Park, O. O. *J. Polym. Sci., Polym. Phys.* **2000**, *38*, 3001–3008.
(57) Wu, F. S.; Woo, E. M. *Polym. Eng. Sci.* **1999**, *39*, 825–832.
(58) Wu, H.; Wang, W.; Yang, H. X.; Su, Z. H. *Macromolecules* **2007**, *40*, 4244–4249.
(59) Hong, B. K.; Jo, W. H.; Kim, J. *Polymer* **1998**, *39*, 3753–3757.
(60) Liu, R. G.; Oppermann, W. *Macromolecules* **2006**, *39*, 4159–4167.
(61) Liu, R. G.; Gao, X.; Opperman, W. *Polymer* **2006**, *47*, 8488–8494.
(62) Alexander, L. E. *X-Ray Diffraction Methods in Polymer Science*; Wiley-Interscience: New York, 1969.
(63) Tosaka, M.; Hamada, N.; Tsuji, M.; Kohjiya, S.; Ogawa, T.; Isoda, S.; Kobayashi, T. *Macromolecules* **1997**, *30*, 4132–4136.
(64) Hamada, N.; Tosaka, M.; Tsuji, M.; Kohjiya, S.; Katayama, K. *Macromolecules* **1997**, *30*, 6888–6892.

MA701988W